Dirasat, Pure Sciences, Volume **39**, No. **1**, 2013

Annealing Effects on the Optical Properties of Europium-Doped Tin Oxide Thin Films Prepared by Electron-Beam Evaporation

Bashar I. Lahlouh, Hassan K. Juwhari, and Mohammad H. Kilani *#*

ABSTRACT

Europium doped tin oxide (SnO_x:Eu) thin films were deposited on silicon and quartz substrates by electron-beam evaporation method. The effects of isothermal annealing temperature on both optical transmission and structure were evaluated by UV-Vis and FTIR measurements. The deposited samples were transparent in the visible light region and down to 320 nm for films annealed at 1100 ^{o} C. The optical band-gap energy has been increased from 3.19 eV for the as-deposited samples to 4.29 eV for samples annealed at 1100 ^{o}C. The refractive index of the films is found to decrease with increasing annealing temperature. The FTIR spectra of the electron-beam deposited films showed that the intensity of Sn-O bridging peaks and Eu related bands are enhanced at high annealing temperatures.

Keywords: Tin Oxide, Europium-doped, Optical Thin Films, Rare Earth Doped, Transparent Oxides.

INTRODUCTION

Tin oxide is one of the well-studied transparent conductive oxides and it exhibits good chemical and mechanical stabilities. Rare earth doped oxide materials, including tin oxide, can be used in displays, optical devices, batteries, solid state lasers, and optical sensors (Shen et al., 2010), (Ningthoujam et al., 2007), (Ray et al., 1998), (Morais et al., 2008). Tin oxide has been studied as a crystalline, semi-crystalline and as an amorphous material by many researchers (de Monredon et al., 2002), (Kroneld et al., 2006), while other researchers studied this material as nanoparticles dispersed in different host matrices such as silica (Ningthoujam et al., 2007).

Different deposition techniques were used to deposit tin oxide based materials. These techniques include sputtering, spray pyrolysis, chemical vapor deposition, sol-gel, dip-coating, and evaporation (de Monredon et al., 2002). These techniques differ in their complexity and the quality of the deposited material. Electron-beam evaporation is considered as one of the basic thin film deposition techniques and often results in good quality thin films. Electron-beam evaporation has been widely used to deposit undoped tin oxide thin films on different substrates (Sentilkumar et al., 2010), (Fallah et al., 2007). (Fallah et al., 2007), (Choudhary et al., 2004). To the authors knowledge, no work was reported on the europium doped tin oxide (SnO_x:Eu) thin films deposited by electron-beam evaporation technique.

This work describes the preparation of Europium-doped tin oxide (SnO_x:Eu) thin films deposited using electron-beam evaporation method. The structure and optical properties of the obtained SnO_x:Eu thin films are also studied and discussed.

EXPERIMENTAL

Europium doped tin oxide evaporation source material was prepared by adding europium salts as nitrates, Eu $(NO_3)_3$:$5H_2O$ (Aldrich, 99.9%), to pure tin metal (Johnson Matthey Chemicals, Puratronic, 99.9985%). The mixture was then thermally treated in air, taken from room temperature (RT) to 700 ºC at a heating rate of 5 ºC per minute and held there for 2 hours. This process produced a white, ceramic-like material with a europium doping level that did not exceed 0.5 % as was estimated qualitatively from EDX (not discussed in this work). The resulting material was then evaporated onto p-

* Department of Physics(1,2); and Department of Chemistry(3), University of Jordan. Received on 25/6/2012 and Accepted for Publication on 8/10/2012.

type (100) silicon (Si) and quartz substrates, held at room temperature, using electron beam evaporation system (SCT- 1800, System Control Technologies). During the deposition processes, the substrates were fixed to a rotating substrate holder placed 60 cm away from the evaporation source. Combination of roughing and cryogenic vacuum pumps was used to pump down the system for 12 hours to arrive at a base pressure of 6×10^{-6} torr before depositing the thin films. The as-deposited SnO_x:Eu thin films were then split into patches and were isothermally annealed in air for 2 hours at different temperatures T_a (200 ^oC, 400 ^oC, 500 ^oC, 600 ^oC,800 ^oC, and 1100 ^oC).

The optical transmission spectra of the as-deposited and annealed samples were recorded using a Shimadzu UV-1601PC UV-Vis spectrophotometer. FilmTek 3000 thin film metrology tool was used to measure the thickness and refractive index of the studied films. Thermo Nicolet NEXUS 670 ™ FTIR Spectrophotometer was used to collect the FTIR spectra of all the samples deposited onto the Si substrates. All measurements were taken at room temperature and under the same equipment settings.

RESULTS AND DISCUSSION

The optical transmittance of the as-deposited and annealed samples (at 500, 600 and 1100 ^oC) is presented in Fig. 1. The transmittance spectra show that the SnO_x:Eu samples are transparent in the visible region of the electromagnetic spectrum. The absorption coefficient $\alpha(h\nu)$ can be written as a function of the energy ($h\nu$) of the incident radiation (Fallah et al., 2007), (Choudhary et al., 2004), (Majumder, 2009)

$$\alpha(h\nu) = (B/h\nu)\,(h\nu - E_g)^r \qquad \ldots(1)$$

where B is a material dependent constant, ν is the frequency of the incident radiation, r is a constant determined by the type of the interband electronic transition. The values of r are taken as 1/2 and 3/2 for allowed and forbidden direct interband transitions and r = 2 and 3 for allowed and forbidden indirect interband transitions (Fallah et al., 2007). Finally, E_g is the optical band-gap energy of the material under study (Fallah et al., 2007), (Choudhary et al., 2004), (Majumder, 2009). The nature of the electronic transition for tin oxide is a matter of controversy; it was considered as a direct-transition process in some studies (Majumder, 2009), (Chen S. et al., 2012), (Nogami et al., 2002), and as an indirect-transition process in other studies (Wang et al., 2010). In this work SnO_x:Eu is treated as a direct band-gap material with r = 1/2. The values of E_g can then be found by extrapolating the linear region of the $(\alpha h\nu)^2$ versus $h\nu$ curves.

To calculate the band gap energy for SnO_x:Eu films, Equation (1) was considered. Fig. 2 shows a plot of $(\alpha h\nu)^2$ versus $h\nu$ for the as-deposited and isothermally annealed SnO_x:Eu samples. The band-gap energies of the studied samples can be calculated by extrapolating the linear region in Fig. 2 and by examining the intersections of the extrapolated lines with the energy axis, where $E_g = h\nu$. The values for E_g were found to vary between 3.19 eV for the as-deposited films at room temperature to 4.29 eV for the samples isothermally annealed at 1100 ^oC.

Fig. 3 summarizes how the band-gap energy varies with isothermal annealing in air. It can be seen that the E_g value increases with annealing temperature. The values of E_g are consistent with the values reported in literature for SnO_x:Eu films produced by other deposition methods (Fallah et al., 2007), (Choudhary et al., 2004), (Majumder, 2009), (Chen S. et al., 2012), (Nogami et al., 2002), (Wang et al., 2010) .The observed absorption in these samples corresponds to the Eu^{3+} ions, and the increased absorption at lower wavelengths may be attributed to the precipitation of small size SnO_x crystals as the annealing temperature is increased. Similar behavior was reported by other researchers (Fallah et al., 2007), (Nogami et al., 2002).

The refractive index and thickness of SnO_x:Eu films were measured from the analysis of the experimental spectral reflectance for the films deposited on silicon. Fig. 4 shows the measured spectral reflectance of the as-deposited sample at room temperature. The experimental reflectance spectra for all measured films were fitted using the FilmTek software package provided with the spectrometer. The generalized Lorentz oscillator model (SCI-Model, Scientific Computing International) was used to fit for the refractive index of the studied films. The refractive index, measured at 632 nm wavelength and at room temperature, was observed to decrease as the annealing temperature was increased for SnO_x:Eu films studied in this work. This behavior of the refractive index is shown in Fig. 5. The measured refractive index values are consistent with the values of SnO_x:Eu films produced by other methods (Goldsmith et al., 2009), (Jumg et al., 2004). The change in the refractive index

can be attributed to structural changes that occur at different annealing temperatures as the band-gap and refractive index dependence on annealing temperature may suggest.

The structure of SnO_x:Eu films had been also evaluated by measuring and comparing the FTIR spectra for the as-deposited and annealed films. Fig. 6 shows a comparison of the FTIR spectra for the studied films. The region above 1350 cm^{-1} did not show any peaks except for the as-deposited sample, where a small band centered around 3300 cm^{-1} was observed. This band is the typical –OH vibration band (Fu et al., 2005).

The FTIR spectra of the as-deposited and annealed at 200^oC films were close to each other with a wide absorption band centered around the region extending from 400 cm^{-1} to 650 cm^{-1}. This band corresponds to a region of Sn-O oscillations (Gu et al., 2003), (Chen D. et al., 2004), (Chen J. etal.,2008). The FTIR spectra of the as-deposited and 200^oC annealed SnO_x:Eu films also show two peaks in the vicinity of 420 cm^{-1} and 1100 cm^{-1}. The 1100 cm^{-1} can be attributed to Eu-bonding (Jumg et al., 2004), but the peak in the vicinity of 420 cm^{-1} was not observed by other workers. For the films annealed at higher temperatures (400 ^oC, 500^oC, 600 ^oC, 800 ^oC, and 1100 ^oC) other absorption peaks, which were not observed in other works, also appeared, in particular the peaks near 470 cm^{-1} and 490 cm^{-1}. The origin of these peaks can be explained by the fact that electron-beam evaporation tends to fragment the evaporated source material which leads to formation those new bonds in the resulting SnO_x:Eu films (Mattox, 1998), (Sree Harsha, 2006). A closer look at the new peaks is illustrated in Fig. 7 which depicts the absorption coefficient as a function of the wavenumber of the IR radiation. The intensity of the new observed peaks reduced as the annealing temperature is increased, while the intensity of the peaks near 580 cm^{-1} and 610 cm^{-1} increased. The latter two absorption peaks can be attributed to Sn-O and Sn-O-Sn stretching, respectively (Fu et al., 2005), (Gu et al., 2003). The peak observed near 530 cm^{-1} and the shoulder near 650 cm^{-1} are also attributed to Sn-O vibrations (Sambasuvam et al., 2010).

Moreover, as the annealing temperature increased the intensity of the absorption peaks near 1100 cm^{-1} sharply increased. These peaks are attributed to Eu vibrations (Sambasuvam et al., 2010). At high annealing temperatures, Eu is allowed to diffuse into the SnO_x bulk where it gets incorporated into the SnO_x matrix. The change in the intensities and the positions of the different peaks in the FTIR spectra is a direct indication of the structural evolution of the isothermally annealed films and this fact was also reflected in the behavior of both the refractive index and the band-gap energy discussed earlier.

CONCLUSIONS

Electron-beam evaporation technique is a viable choice for depositing high quality SnO_x:Eu thin films. Annealing SnO_x:Eu films at temperatures higher than 800^oC can improve their structure substantially. At such elevated temperatures, Eu is allowed to diffuse well into the SnO_x matrix and it is allowed to enter the structure of the material as was observed in the FTIR spectra. Isothermal annealing at high temperatures also improved the transparency of the SnO_x:Eu films, with the films annealed at 1100 ^oC were more transparent to UV radiation compared to films annealed at lower temperatures. This fact was reflected in the band-gap measurement where the band-gap energy increased from 3.19 eV for the as-deposited films to 4.29 eV for films annealed at 1100 ^oC.

ACKNOWLEDGEMENTS

This research is financially supported by the Deanship of Academic Research at the University of Jordan (project number 1064).

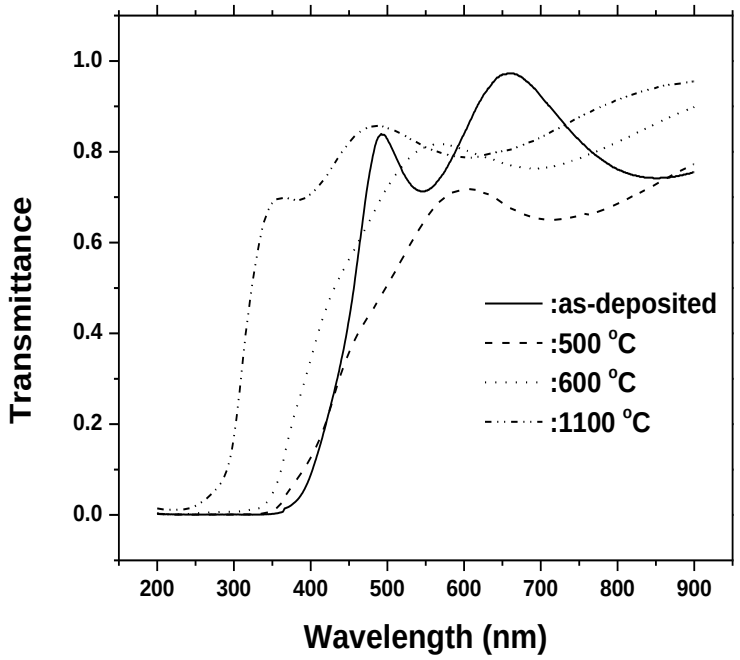

Fig. 1. The optical transmittance spectra of the as-deposited and annealed SnO_x:Eu thin films.

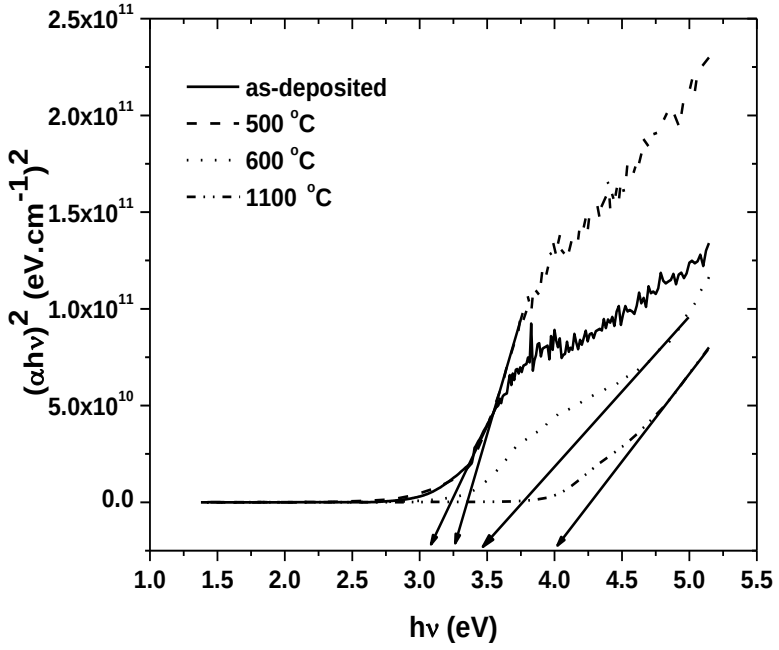

Fig. 2. $(\alpha h\nu)^2$ versus hν for the as-deposited SnO_x:Eu film and SnO_x:Eu films annealed in air at different temperatures.

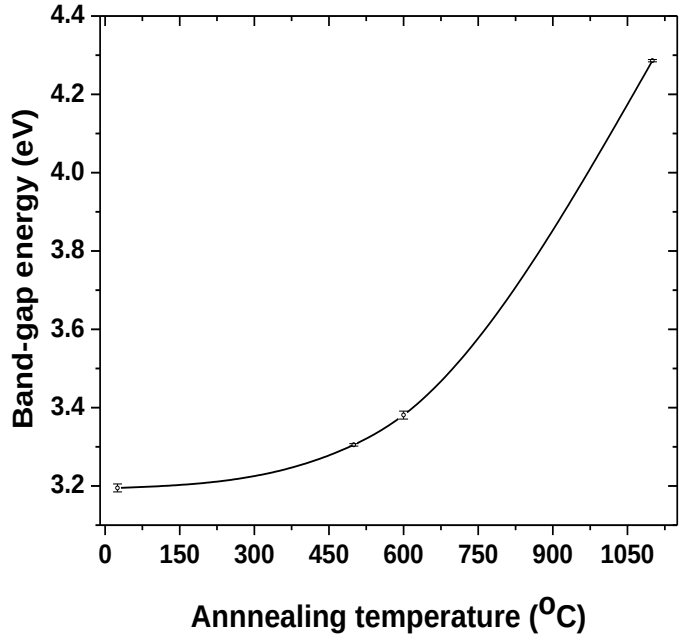

Fig. 3. Variation of the band-gap energy of SnO_x:Eu films with isothermal annealing temperature.

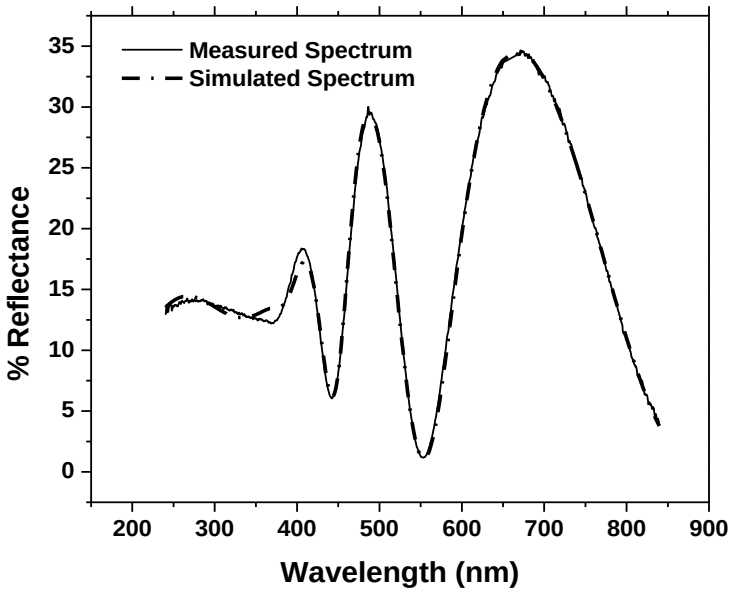

Fig. 4. Measured and simulated reflectance spectrum of the as-deposited SnO_x:Eu film.

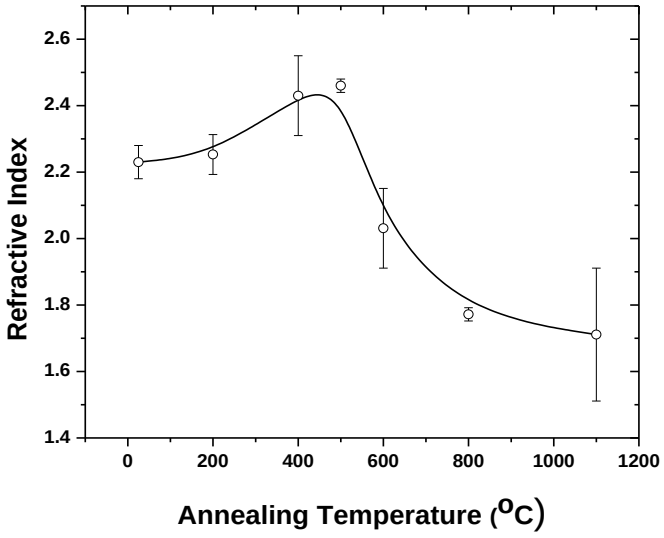

Fig. 5. A plot of the variation of index of refraction with isothermal annealing temperature for SnO_x:Eu film .

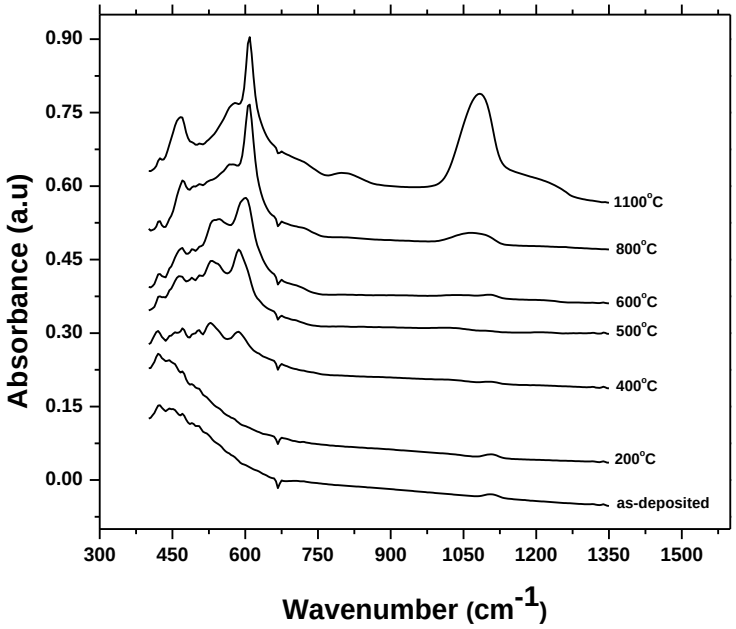

Fig. 6. FTIR spectra of the as-deposited and annealed SnO_x:Eu films.

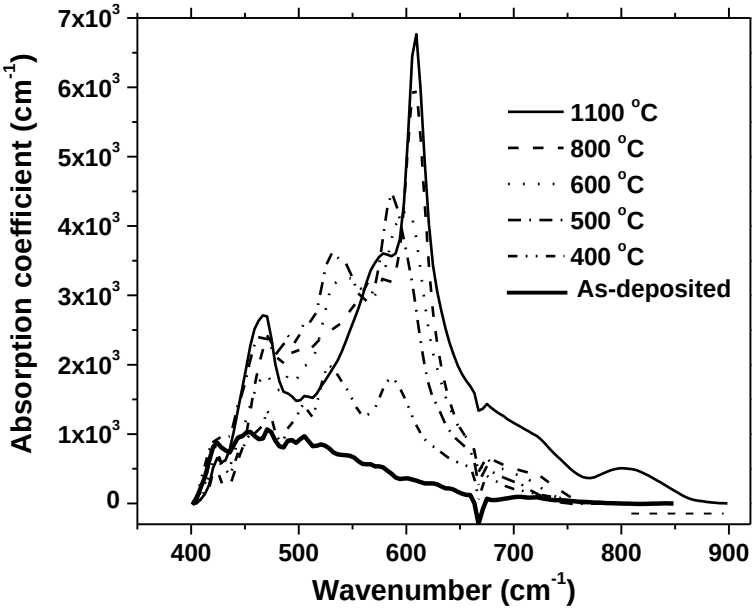

Fig. 7. Absorption coefficient versus wavenumber for the as-deposited and annealed SnO_x:Eu films in the near infrared region.

REFERENCES

Ce Shen, S. Baccaro, Zhongwen Xing, Qiqi Yan, Shufen Wang, Gurong Chen. 2010. *Chem. Phys. Lett*., 492, 123-126.

Choudhary, R. J., Ogale, S. B., Shinde, S. R., Kulkarni, V. N., Venkatesan, T., Harshavardhan, K. S., Strikovski, M., Hannoyer, N. 2004. *Appl. Phys. Lett*. 84 (9), 1483-1485.

Deliang Chen, Lian Gao. 2004. *J. Colloid Interface Sci*. 279, 137-142.

Donald, M. Mattox. 1998. *Handbook of Physical Vapor Deposition (PVD) Processing*, Noyes Publications, 301.

Evandro A. Morais, Luis V. A. Scalvi, Americo Tabata, Jose B. B. De Oliveira, Sidney J. L. Ribeiro. 2008. *J. Mater. Sci*., 43:345-349.

Feng, Gu, Shu Fen Wang, Chun Feng Song, Ming Kai Lu, Yong Xin Qi, Guang Jun Zhou, Dong Xu, Duo Rong Yuan. 2003. *Chem. Phys. Lett*. 372, 451-454.

Goldsmith, S., Cetinorgu, E., Boxman, R.L. 2009. *Thin Solid Films*, 517, 5146-5150.

Guofeng, Wang, Yiping Yang, Quiying Mu, Yude Wang, 2010, *J. Alloys Compd*. 498, 81-87.

Hamid Reza Fallah, Mohsen Ghasemi, Ali Hassanzadeh, Hadi Steki. 2007. *Mater. Res. Bull*. 42, 487-496.

Hamid Reza Fallah, Mohsen Ghasemi, Ali Hassanzadeh. 2007. *Physica E 39*, 69-74.

Jiangtao Chen, Jun Wang, Fei Zhang, De Yan, Guangan Zhang, Renfu Zhuo. Pengxun yan. 2008. *J. Phys. D: Appl. Phys*. 41, 105306.

Kroneld, M., Novikov, S., Saukko, S., kuivalainen, P., Kostamo, P., Lantto, V. *Sens. Actuators*. 2006. B 118, 110-114.

Majumder, S. 2009. *Mater. Sci.- Pol*. 27, (1), 123-129.

Masayuki Nogami, Takehiro Enomoto, Tomokatsu Hayakawa, J. Lumin. 97 (2002) 147-152.

Ningthoujam, R.S., Sudarsan, V., Kulshreshtha, S.K., Lumin. J. 2007. 127, 747-756.

Sambasuvam, S., Saes Byul Kim, Jung Hyun Jeong, Byng Chun Choi, Kwon Taek Lim, Sang Su Kim, Tae Kwon Song. 2010. *Curr. Appl. Phys*. 10, 1383-1386.

Sekhar C. Ray, Malay K. Karanji, Dhruba DasGupta. 1998. *Surf. Coat. Technol*., 102, 73-80.

Senthilkumar, V., Vickraman, P. 2010. *J. Mater. Sci*.: *Mater. Electron*., 21:578-583.

Shuai Chen, Xiaoru Zhao, Haiyan Xie, Jinming Liu, Libing Duan, Xiaojun Ba, Jianlin Zhao. 2012. *Appl. Surf. Sci*. 258, 3255-3259.

Sophie de Monredon, Antoine Cellot, Francois Ribot, Clement Sanchez, Lidia Armelao, Lethicia Gueneau,

Laurent Delattre. 2002. *J. Mater Chem*., 12, 2396 -2400.
Sree Harsha, K. S. 2006. *Principles of Physical Vapor Deposition of Thin Films*, First Edition, ELSEVIER, 49.
Xiaoyan, Fu, Hongwu Zhang, Shuyun Niu, Qin Xin. 2005. J. Solid State Chem. 178, 203-607.
Yeon, Sik Jumg. 2004. *Thin Solid Films*, 467, 36-42.

تأثير التسخين على الخواص الضوئية لأغشية أكسيد القصدير المطعم باليوروبيوم والمحضَر بأستخدام طريقة التبخير بشعاع الألكترونات

بشار إبراهيم لحلوح، حسان خالد الجوهري، ومحمد حسين كيلاني *

ملخص

تم ترسيب أغشية أكسيد القصدير المطعم باليوروبيوم على ركائز السيليكون والكوارتز بأستخدام طريقة التبخير بشعاع الألكترونات. يتناول البحث تأثير التسخين تحت درجة حرارة ثابتة على كل من الإنفاذ الضوئي والتركيب باستخدام مطيافيتي الأشعة فوق البنفسجية و ما تحت الحمراء. أظهرت العينات نفاذية عالية للضوء المرئي بشكل متزايد حتى وصلت الى إنفاذ الضوء عند 320 نانومتراً عند حرارة تسخين تعادل 1100 درجة مئوية. طاقة الفجوة الضوئية تزايدت من 3.19 إلكترون فولت للعينات غير المسخنة ووصلت إلى 4.29 إلكترون فولت للعينات المسخنة عند 1100 درجة مئوية، كما لاحظت الدراسة تزايد معامل الأنكسار مع زيادة حرارة التسخين. أظهرت مطيافية الأشعة تحت الحمراء انه مع زيادة حرارة التسخين فإنه يمكن ملاحظة تزايد في شدة الطيف في مناطق الترددات الخاصة باكسيد القصدير وروابط اليوروبيوم.

الكلمات الدالة: أكسيد القصدير، التطعيم باليوروبيوم، أغشية ضوئية، التطعيم بالمعادن الأرضية النادرة، الأكاسيد المنفذة للضوء.

* قسم الفيزياء(1، 2)، وقسم الكيمياء(3)، الجامعة الأردنية. تاريخ استلام البحث 2012/6/25 وتاريخ قبوله 2012/10/8.